

RV variable, hot post-AGB stars from the MUCHFUSS project

- Classification, atmospheric parameters, formation scenarios

N. Reindl¹, S. Geier^{2,3,4}, T. Kupfer⁵, S. Bloemen⁶,
V. Schaffenroth^{7,3}, U. Heber³, B. N. Barlow⁸, and R. H. Østensen⁹

¹ Institute for Astronomy and Astrophysics, Kepler Center for Astro and Particle Physics, Eberhard Karls University, Sand 1, 72076, Tübingen, Germany

e-mail: reindl@astro.uni-tuebingen.de

² Department of Physics, University of Warwick, Coventry CV4 7AL, UK

³ Dr. Karl Remeis-Observatory & ECAP, Astronomical Institute, Friedrich-Alexander University Erlangen-Nuremberg, Sternwartstr. 7, D 96049 Bamberg, Germany

⁴ ESO, Karl-Schwarzschild-Str. 2, 85748 Garching bei München, Germany

⁵ Division of Physics, Mathematics, and Astronomy, California Institute of Technology, Pasadena, CA 91125, USA

⁶ Department of Astrophysics/IMAPP, Radboud University Nijmegen, P.O. Box 9010, 6500 GL Nijmegen, The Netherlands

⁷ Institute for Astro- and Particle Physics, University of Innsbruck, Technikerstr. 25/8, 6020 Innsbruck, Austria

⁸ Department of Physics, High Point University, 833 Montlieu Avenue, High Point, NC 27262, USA

⁹ Institute of Astronomy, KU Leuven, Celestijnenlaan 200D, B-3001 Heverlee, Belgium

Received – Accepted –

ABSTRACT

In the course of the MUCHFUSS project we have recently discovered four radial velocity (RV) variable, hot ($T_{\text{eff}} \approx 80\,000\text{--}110\,000\text{ K}$) post-asymptotic giant branch (AGB) stars. Among them, we found the first known RV variable O(He) star, the only second known RV variable PG 1159 close binary candidate, as well as the first two naked (i.e., without planetary nebula (PN)) H-rich post-AGB stars of spectral type O(H) that show significant RV variations. We present a non-LTE spectral analysis of these stars along with one further O(H)-type star whose RV variations were found to be not significant. We also report the discovery of an far-infrared excess in the case of the PG 1159 star. None of the stars in our sample displays nebular emission lines, which can be explained well in terms of a very late thermal pulse evolution in the case of the PG 1159 star. The “missing” PNe around the O(H)-type stars seem strange, since we find that several central stars of PNe have much longer post-AGB times. Besides the non-ejection of a PN, the occurrence of a late thermal pulse, or the re-accretion of the PN in the previous post-AGB evolution offer possible explanations for those stars not harbouring a PN (anymore). In case of the O(He) star J0757 we speculate that it might have been previously part of a compact He transferring binary system. In this scenario, the mass transfer must have stopped after a certain time, leaving behind a low mass close companion that could be responsible for the extreme RV shift of $107.0 \pm 22.0\text{ km/s}$ measured within only 31 min.

Key words. binaries: spectroscopic – stars: AGB and post-AGB – stars: evolution – stars: atmospheres

1. Introduction

The discovery and analysis of close binaries throughout all evolutionary stages plays an important role in various astronomical fields. Due to the radiation of gravitational waves, very close (periods less than a few hours) binary systems may merge within a Hubble time. If the system contains two sufficiently massive white dwarfs or a subdwarf star and a sufficiently massive white dwarf, this evolutionary path can lead to a type Ia supernova (Webbink 1984), the so-called double degenerate scenario. If the total mass of the two merging stars does not exceed the Chandrasekhar limit, He-dominated stars, i.e., R Coronae Borealis stars (RCB), extreme helium (EHe) stars, He-rich subdwarf O (He-sdO) stars or O(He) stars may be produced (Webbink 1984; Iben & Tutukov 1984; Justham et al. 2011; Zhang & Jeffery 2012b,a; Zhang et al. 2014; Reindl et al. 2014b). The existence of planetary nebulae (PNe) around every other O(He) star and the [WN] type central stars, however, questions the possibility that all He-dominated stars have a merger origin. Those stars might have lost their H-rich envelope via enhanced mass-loss

during their post-asymptotic giant branch (AGB) evolution, possibly triggered by a close companion (Reindl et al. 2014b).

Close binary evolution is also needed to explain the formation of low mass He-core white dwarfs ($M < 0.5 M_{\odot}$), because the evolutionary time-scale of the supposed low-mass single main-sequence progenitor stars significantly exceeds the Hubble time. The orbital energy released during a common envelope phase, is supposed to rapidly expel the envelope of the pre-low mass white dwarf and may terminate the growth of the He-core before it reaches a sufficient mass for He ignition (Paczynski 1976; Webbink 1984; Iben & Tutukov 1986).

Also the formation of hot subdwarfs (sdO/B), located at the (post-) extreme horizontal branch, may best be understood in terms of close binary evolution. The progenitors of these stars are expected to have undergone a strong mass-loss already on the red giant branch (RGB), which was likely triggered by the close companion. If the mass-loss was sufficiently high, these stars leave the RGB and ignite He only while evolving to or descending the white dwarf cooling curve, and will consequently, reach a hotter zero-age horizontal position (Brown et al. 2001;

Lanz et al. 2004).

Finally, close binaries are proposed to play a crucial role in the formation of asymmetrical PNe, which make up the great majority (80–85%, Parker et al. 2006) of all PNe. The so-called binary hypothesis (De Marco et al. 2009) states that a companion is needed to account for the non-spherical shapes of these PNe. Several research groups are trying to determine the frequency of binary central stars of PNe (CSPNe) and the properties of these systems. Most of the known close binary CSPNe were detected via periodic flux variability due to eclipses, irradiation, and/or ellipsoidal deformation (Bond 2000; Miszalski et al. 2009). This technique is, however, biased against binaries with periods longer than about two weeks, against binaries with low inclination angles, and against companions with small radii (De Marco et al. 2008). Large radial velocity (RV) surveys of CSPNe are telescope-time expensive and not always straightforward, because most of the strongest photospheric lines are blended with nebular emission lines and the extraction of the pure stellar spectrum may often not be successful in the case of very compact nebulae.

Fortunately, several hundreds of hot subluminal stars, which generally do not display nebular lines, were observed in the course of the Sloan Digital Sky Survey (SDSS). Because SDSS spectra are co-added from at least three individual integrations (with a typical exposure time of 15 min), they offer the ideal basis for the search for RV variations. The MUCHFUSS (Massive Unseen Companions to Hot Faint Underluminal Stars from SDSS) survey made use of that to search for hot subdwarf stars with massive compact companions (Geier et al. 2011). For that purpose, hot subdwarfs were selected from the SDSS DR7 by color (i.e., they were required to be point sources with $u - g < 0.4$ and $g - r < 0.1$) and visual inspection of their spectra in order to distinguish them from hot white dwarfs or extragalactic sources. Those stars, whose SDSS sub-spectra revealed high RV variations, were selected as candidates for follow-up spectroscopy to derive the RV curves and the binary mass functions of the systems. In this way, more than 100 RV-variable subdwarfs have been found (Geier et al. 2015).

Hot post-AGB stars directly overlap with hot subdwarfs of O-type (sdO) in the color-color plane. If hot post-AGB stars are not surrounded by a compact nebula and/or do not suffer from still ongoing strong mass loss (i.e., weak emission line stars, Wolf Rayet type central stars, whose spectra show or are even dominated by emission lines), their spectra may look indistinguishable from the less luminous sdO stars. About three-quarter of all hot post-AGB stars display a normal H-rich composition and in case their spectra are dominated by absorption lines, they can be classified as O(H) or hgO(H) stars (the latter case applies to high gravity stars which are positioned on the white dwarf cooling track, Mendez 1991). Hot, H-deficient stars, which show predominantly absorption lines and lie in the post-AGB region, are either classified as O(He) stars (typically showing more than 90% He, by mass), or PG 1159 stars, whose spectra show besides He also strong lines of carbon. By eye, the spectra of O(H), O(He), and PG 1159 stars may look very similar to those of the less luminous sdO, He-sdO, and C-strong lined He-sdO stars, respectively. Thus, the sample of Geier et al. (2015) also contains a small fraction of hot post-AGB candidates, namely SDSS J075732.18+184329.3 (here after J0757), SDSS J093521.39+482432.4 (J0935), SDSS J100019.98-003413.3 (J1000), SDSS J155610.40+254640.3 (J1556), and SDSS J204623.12-065926.8 (J2046). Previous analyses of these stars indicated very high effective temperatures (Werner et al. 2014; Geier et al. 2015). Because of the rareness of such objects

as well as their importance for our understanding of the late, hot stages of stellar evolution we decided to subject these five stars to a more comprehensive analysis and discussion of their evolutionary status.

The paper is organized as follows. First, we describe the observations and the discovery of RV variations (Sect. 2). Then, we determine the parameters of the stars in Sect. 3. In Sect. 4 follows a search for a PN and an infrared excess. The evolutionary status of the stars is discussed in Sect. 5 and finally we conclude in Sect. 6.

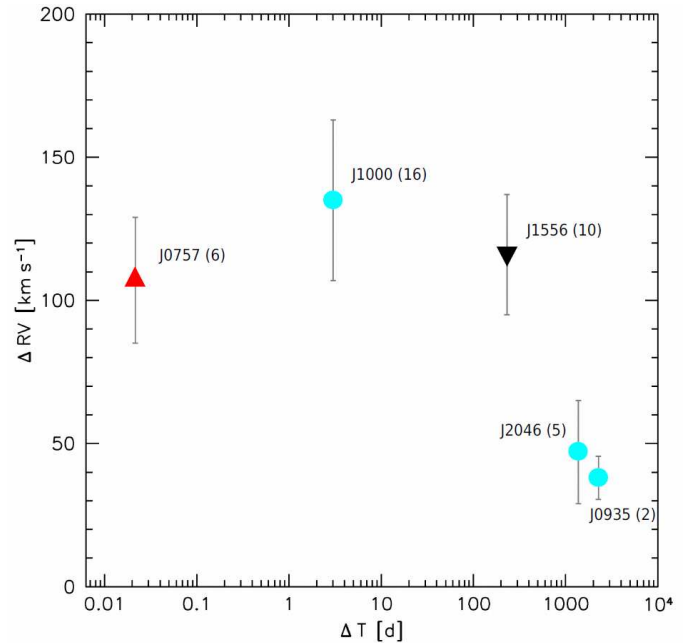


Fig. 1. Highest RV shift between individual spectra plotted against time difference between the corresponding observing epochs for the O(He) star J0757 (red, triangle), the PG1159 star J1556 (black, inverted triangle), and the three O(H) stars J1000, J2046, and J0935 (blue, filled circles). The numbers in the brackets correspond to the number of epochs each star was observed. Note that the RV shifts of J2046 were found to be not significant.

2. Observations and detection of radial velocity variations

Individual observations and RV measurements of the five stars are listed in Geier et al. (2015). The RVs were measured by fitting a set of mathematical functions (Gaussians, Lorentzians, and polynomials) to the spectral lines using the FITSB2 routine (Napiwotzki et al. 2004). The fraction of false detections produced by random fluctuations and the significance of the measured RV variations were calculated as described in Maxted et al. (2001).

In the spectra of J0757, J0935, J1000, and J1556 we discovered significant RV shifts, while the RV variations in the five SDSS sub-spectra of J2046 were found to be most likely caused by random fluctuations (false-detection probability p is larger than 0.01%). In Fig. 1 we show their highest RV shift between individual spectra plotted against time difference between the corresponding observing epochs. Most impressive, we discovered a maximum RV shift of 107.0 ± 22.0 km/s within only 31 min in the six SDSS sub-spectra (taken in two consecutive nights) of J0757. J1000 was observed 16 times in the course of the SDSS and reveals a maximum RV shift of 135.0 ± 28.0 km/s. In addition to the

nine SDSS observations of J1556, we have obtained one medium resolution spectrum with TWIN at the Calar Alto 3.5 m telescope and found a maximum RV shift of 116.0 ± 21.0 km/s. For J0935 second epoch spectroscopy was obtained with WHT/ISIS. The maximum RV shift is 38.0 ± 7.5 km/s.

To verify the close binary nature of the stars, we tried to derive orbital periods and RV semiamplitudes of the objects with more than ten epochs as described in Geier et al. (2015). Unfortunately, in both cases the RV datasets were insufficient to put any meaningful constraints on the orbital parameters.

3. Stellar parameters and distances

In this section we first perform a non-LTE spectral analysis to derive the effective temperatures, surface gravities and the chemical composition of the five stars (Sect. 3.1). These parameters are then used in Sect. 3.2 to derive their masses, luminosities, and distances.

3.1. Spectral analysis

Quantitative spectral analysis is the key to derive the surface parameters of the stars and to understand their evolutionary status. Our spectral analysis was based on the SDSS observations of the stars. The single spectra have been corrected for their orbital motion and coadded. For the model calculations we employed the Tübingen non-LTE model-atmosphere package (TMAP¹, Werner et al. 2003; Rauch & Deetjen 2003) which allows to compute plane-parallel, non-LTE, fully metal-line blanketed model atmospheres in radiative and hydrostatic equilibrium. Model atoms were taken from the Tübingen model atom database TMAD². To calculate synthetic line profiles, we used Stark line-broadening tables provided by Barnard et al. (1969) for He I $\lambda\lambda$ 4026, 4388, 4471, 4921 Å, Barnard et al. (1974) for He I λ 4471 Å, and Griem (1974) for all other He I lines. For He II we used the tables provided by Schönig & Butler (1989), for H I tables provided by Tremblay & Bergeron (2009), and for C IV tables provided by Dimitrijević et al. (1991) and Dimitrijević & Sahal-Brechot (1992).

3.1.1. H-rich stars

The spectra of J0935, J1000, and J2046 are dominated by hydrogen Balmer lines. Spectral lines of He II are of moderate strength, but no He I lines can be detected. However, the signal to noise of the observations is too poor ($S/N \approx 20$ -30) to exclude their presence from the outset. To derive effective temperatures, surface gravities, and He abundances of these stars, we calculated a model grid spanning from $T_{\text{eff}} = 40\,000 - 140\,000$ K (step size 1250 K) and $\log g = 4.75 - 6.5$ (step size 0.25 dex) for six different He abundances (He = 0.1, 0.2, 0.3, 0.4, 0.5, and 0.6, by mass). Models above the Eddington limit (i.e., $T_{\text{eff}} > 90\,000$ K for $\log g = 4.75$, $T_{\text{eff}} > 100\,000$ K for $\log g = 5.00$, and $T_{\text{eff}} > 120\,000$ K for $\log g = 5.25$) were not calculated. For He II 20 levels were considered in non-LTE, and for He I 29 levels if $T_{\text{eff}} < 100\,000$ K, and 5 levels if $T_{\text{eff}} \geq 100\,000$ K. For H I 15 levels were considered in non-LTE. The parameter fit was then performed by means of a χ^2 minimization technique with SPAS (Spectrum Plotting and Analysing Suite, Hirsch 2009), which is based on the FITSB2 routine (Napiwotzki 1999). We fitted

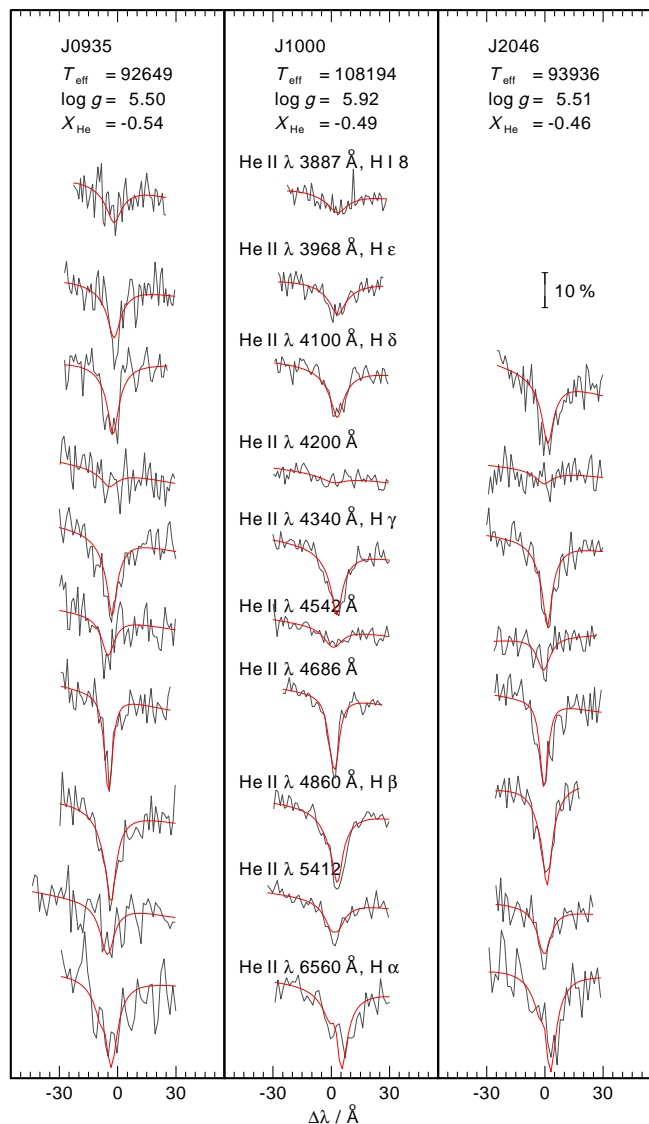


Fig. 2. Balmer and He II lines used to derive T_{eff} , $\log g$, and the He abundance (given in logarithmic mass fractions) of the three O(H)-type stars. The observations are shown in grey, the best fit models in black (red in online version). The vertical bar indicates 10% of the continuum flux.

all Balmer and He II lines detected in the SDSS spectra of these stars. He II λ 3968 Å/H ϵ and He II λ 3887 Å/H I λ 3889 Å were not fitted in case of J2046 due to the poor quality of the blue part of the spectra. Our best fits are shown Fig. 2 and the results of our analysis are summarized in Table 1.

The spectra were previously analysed by Geier et al. (2015) based on a model grid calculated by Stroeger et al. (2007) and we find that they generally underestimated T_{eff} by 5 to 15%. In addition, our results for J1000 lie outside the grid used by Geier et al. (2015). While the effects of the smaller step size in T_{eff} (1250 K instead of 5000 K) of our grid, are relatively small (T_{eff} is usually underestimated by 1% when using a finer grid), the main influence can be attributed in the larger extent towards higher T_{eff} (140 000 K instead of 100 000 K), as well as in the use of the Stark line-broadening tables provided by Tremblay & Bergeron (2009) instead of those provided by Lemke (1997).

It is important to note, that the errors given in Table 1 correspond to formal fitting errors only. The neglect of metal opacities in the model-atmosphere calculations can lead to significant sys-

¹ <http://astro.uni-tuebingen.de/TMAP>

² <http://astro.uni-tuebingen.de/TMAD>

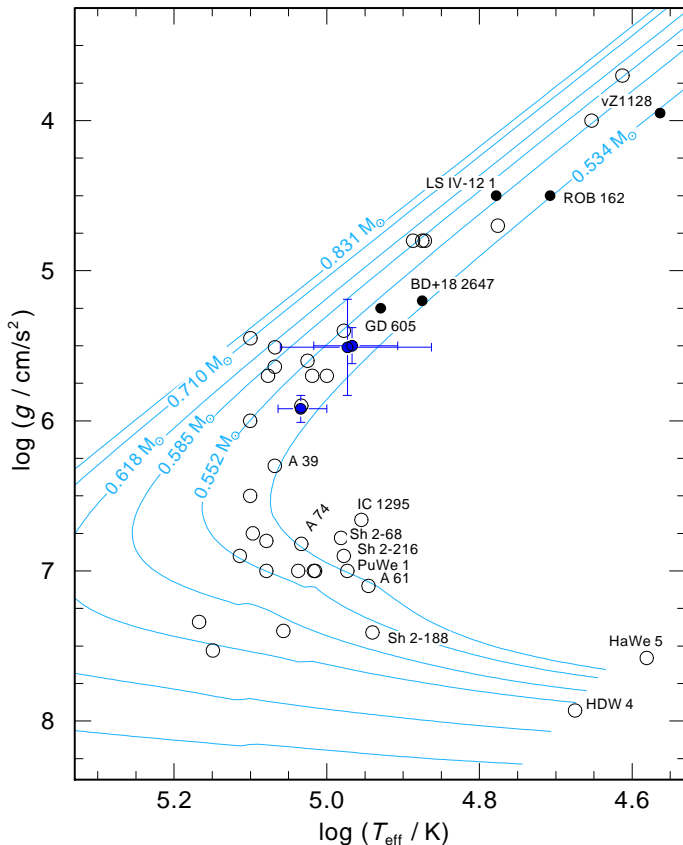


Fig. 3. The locations of our three O(H) stars (filled, blue circles with error bars) are compared with H-burning post-AGB evolutionary tracks (blue lines, labeled with stellar masses, Miller Bertolami 2015). Also shown are the locations of naked O(H)-type stars (filled circles, Chayer et al. 2015; Fontaine et al. 2008; Bauer & Husfeld 1995; Heber & Hunger 1987; Heber & Kudritzki 1986), as well as the locations of H-rich CSPNe (open circles, Ziegler 2012; Herald & Bianchi 2011; Gianninas et al. 2010; Rauch et al. 2007; Napiwotzki 1999).

tematic errors in the inferred atmospheric parameters of very hot stars. Latour et al. (2010, 2015) showed that for sdO stars hotter than about 70 000 K, T_{eff} and $\log g$ are typically underestimated by 5 to 10% and 0.15 dex, respectively.

However, even considering these effects, all stars lie clearly in the post-AGB region of the $\log T_{\text{eff}} - \log g$ diagram, shortly before they will reach their maximum T_{eff} , to then cool down as white dwarfs (Fig. 3). Their He abundances are slightly supersolar ($1.2 - 1.4 \times$ solar, solar abundance according to Asplund et al. 2009). In order to distinguish these stars from sdO stars, which are usually associated with AGB-manqué stars, which are stars that fail to evolve through the AGB, we employ the spectral classification scheme of Mendez (1991) and classify them as O(H) type stars.

3.1.2. H-deficient stars

J0757 has been analysed by Werner et al. (2014), who derived $T_{\text{eff}} = 80\,000\text{ K}$, $\log g = 5.00$ and a C abundance of $C = 0.006$ (by mass). Thus, the star belongs to the class of C-rich O(He) stars.

The C lines in the spectrum of J1556 are stronger and more numerous compared to the ones found in the spectrum of J0757. In Fig. 4 the co-added SDSS spectrum of J1556 is shown. Besides photospheric lines of He II and C IV, we could identify lines

of N V and O V. Constraints on the effective temperature can already be put from the absence of He I lines ($T_{\text{eff}} \geq 70\,000\text{ K}$) and the C IV $\lambda\lambda 5801, 5812\text{ \AA}$ lines, which appear in emission ($T_{\text{eff}} \geq 90\,000\text{ K}$). In addition, the fact that the N V lines at 4604 \AA and 4620 \AA appear in absorption allows us to put an upper limit of $T_{\text{eff}} \leq 115\,000\text{ K}$ (Rauch et al. 1994).

For the spectral analysis of J1556 we firstly calculated a model grid including only the opacities of H, He, and C. For H and He non-LTE levels were used as described in Sect. 3.1.1. The C model atom includes the ionization stages III-V and 30, 54, and 1 non-LTE levels were considered for C III, C IV, and C V, respectively. Our model grid spans $T_{\text{eff}} = 90\,000 - 120\,000\text{ K}$ and $\log g = 5.0 - 6.7$ and C abundances in the range of 0.33 - 0.01 (by mass) were considered. The grid is, however, not complete due to the occurrence of numerical instabilities. The fitting of the spectrum was then carried out in an iterative process, in which the parameters of the model have been changed successively until a good agreement with the observation was achieved. The best fit was found for $T_{\text{eff}} = 100\,000\text{ K}$, $\log g = 5.33$, and $C = 0.15$. No traces of H could be detected. Unfortunately, we did not succeed in calculating numerically stable models that also included the opacities of N and O at such low surface gravities, which precluded the abundances determination of those elements.

The C abundance lies well above the limit set by Werner et al. (2014) to distinguish between the PG 1159 stars and the He-dominated DO white dwarfs and O(He) stars, which only show up to $C = 0.03$. Therefore, we classify J155610.40+254640.3 as a PG 1159 star. It is worthwhile to note, that this is also the PG 1159 star with the lowest surface gravity known so far. Interestingly, its C abundance is rather low compared to the majority of the luminous PG 1159 stars (that is they have $\log g < 7.0$) which typically show $C = 0.5$ (see Fig. 4 in Reindl et al. 2014a for comparison).

3.2. Masses, luminosities, and distances

To derive the masses and luminosities of the five stars, we compared their position in the $\log T_{\text{eff}} - \log g$ plane with different evolutionary tracks. Figure 3 shows the location of the three O(H) stars compared with H-burning post-AGB evolutionary tracks (Miller Bertolami 2015). Because these stars most likely belong to the Galactic halo (see below), we used tracks with $Z = 0.001$. We derived $M = 0.54 M_{\odot}$ for all O(H)-type stars, which agrees well within the error limits with the mean mass of $0.551 \pm 0.005 M_{\odot}$ of H-rich halo white dwarfs (Kalirai 2012).

In the upper panel of Fig. 5 the locations of the two H-deficient stars, J0757 and J1556, are compared with a late thermal pulse (LTP) evolutionary track of Miller Bertolami & Althaus (2007) and very LTP (VLTP) post-AGB tracks of Miller Bertolami & Althaus (2006). We derived $M = 0.57 M_{\odot}$ for J1556, and $M = 0.53 M_{\odot}$ for J0757. For J0757 we additionally derived the mass and luminosity using post-double He white dwarf merger evolutionary tracks of Zhang & Jeffery (2012a,b) and found $M = 0.73 M_{\odot}$ (lower panel of Fig. 5). Within the error limits, J0757 could also be a merger of a CO white dwarf and a He white dwarf, however, to this date there are no post-CO+He white dwarf merger tracks available that reach to the region of O(He) type stars. We stress that a reliable spectroscopic mass determination for J0757 would only be possible if the evolutionary history of this object would be known. Therefore, the parameter listed for J0757 in Table 1, are only valid if a certain scenario is assumed.

Based on the derived masses, we calculated the distances of

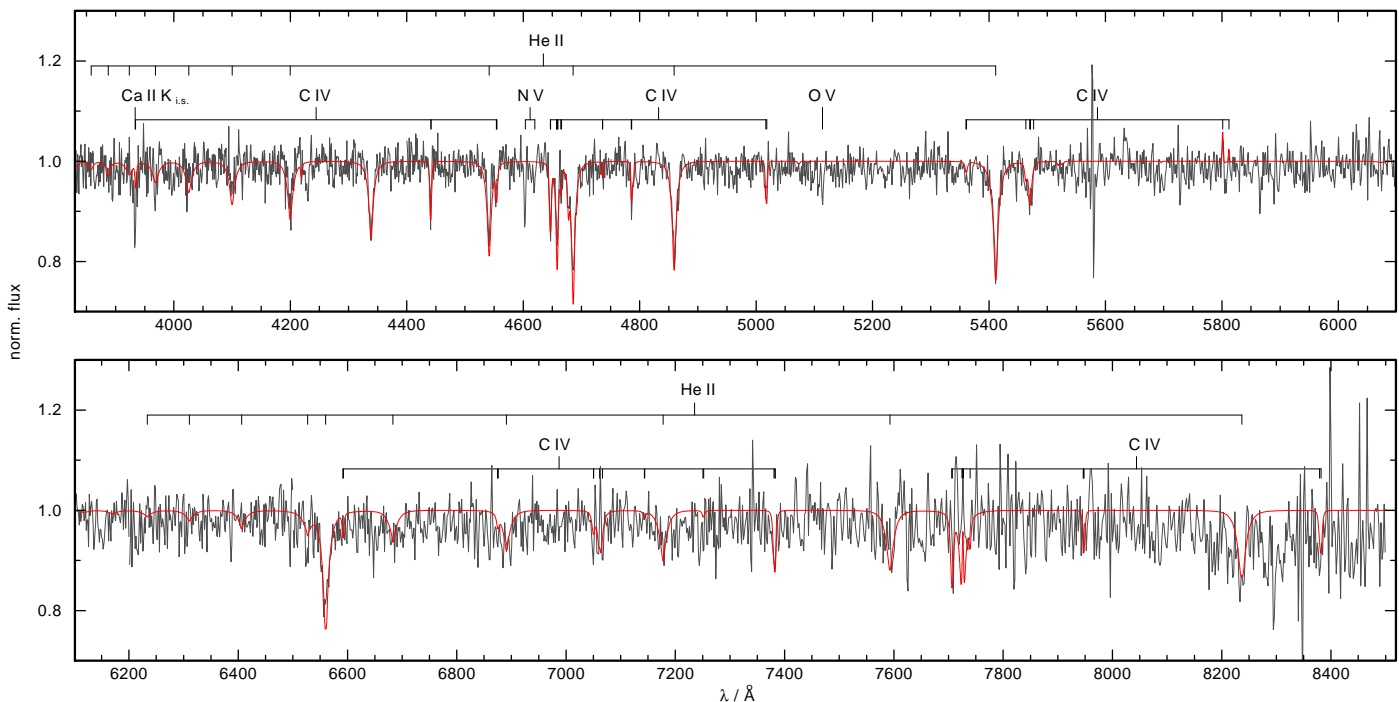


Fig. 4. Coadded and normalized SDSS spectrum (grey) of the PG 1159 star SDSS J155610.40+254640.3. The best fit model (black, red in online version) including He and C lines is superimposed and the positions of identified spectral lines are indicated.

Table 1. Stellar Parameter. He abundances are given in logarithmic mass fractions.

name	Spectral type	T_{eff} [K]	$\log g$	X_{He}	M [M_{\odot}]	$\log(L/L_{\odot})$	d [kpc]	z [kpc]
J0935	O(H)	92649 ± 11358	5.50 ± 0.12	-0.46 ± 0.09	$0.54^{+0.05}_{-0.01}$	$3.5^{+0.4}_{-0.2}$	$16.7^{+2.7}_{-2.2}$	$12.1^{+1.8}_{-1.6}$
J1000	O(H)	108194 ± 8356	5.92 ± 0.09	-0.49 ± 0.06	$0.54^{+0.02}_{-0.01}$	$3.4^{+0.2}_{-0.1}$	$8.0^{+0.9}_{-0.8}$	$5.2^{+0.6}_{-0.5}$
J2046	O(H)	93936 ± 21166	5.51 ± 0.32	-0.54 ± 0.16	$0.54^{+0.08}_{-0.01}$	$3.5^{+0.5}_{-0.2}$	$10.8^{+4.8}_{-3.3}$	$-5.2^{+1.6}_{-2.3}$
J1556	PG 1159	100000^{+15000}_{-10000}	5.30 ± 0.30	-0.07 ± 0.03	$0.57^{+0.13}_{-0.05}$	$3.8^{+0.5}_{-0.4}$	$16.3^{+6.7}_{-4.8}$	$12.3^{+5.1}_{-3.6}$
J0757 ^(a)	O(He)	80000 ± 20000	5.00 ± 0.30	-0.01 ± 0.01	$0.53^{+0.21}_{-0.05}$ ^(a)	$3.7^{+0.6}_{-0.3}$ ^(b)	$26.8^{+11.1}_{-7.8}$ ^(b)	$10.3^{+4.3}_{-3.0}$ ^(b)
					$0.73^{+0.27}_{-0.08}$ ^(c)	$3.9^{+1.0}_{-0.5}$ ^(c)	$31.5^{+13.0}_{-9.2}$ ^(c)	$12.1^{+5.0}_{-3.5}$ ^(c)

Notes.

^(a) Atmospheric parameters taken from Werner et al. (2014). ^(b) Based on (V)LTP tracks of Miller Bertolami & Althaus (2007, 2006). ^(c) Based on double He-white dwarf merger tracks of Zhang & Jeffery (2012a,b).

the stars by using the flux calibration of Heber et al. (1984) for $\lambda_{\text{eff}} = 5454 \text{ \AA}$,

$$d [\text{pc}] = 7.11 \times 10^4 \cdot \sqrt{H_V \cdot M \times 10^{0.4 m_{V_0} - \log g}},$$

with $m_{V_0} = m_V - 2.175c$, $c = 1.47E_{B-V}$, and the Eddington flux H_V at λ_{eff} of the best-fit model atmospheres of each star. Values for E_{B-V} were obtained from Galactic dust extinction maps from Schlafly & Finkbeiner (2011) and values for m_V were taken from Geier et al. (2015). The distances range from 8.0 to 31.5 kpc and deviate slightly from the values listed in Geier et al. (2015). This is because they used different model fluxes and assumed a canonical mass of $0.6 M_{\odot}$ for all post-AGB stars for their distance determination. We found that all five stars are located far above or below the Galactic plane (Table 1). Since the thick disk only dominates in the region $1 \text{ kpc} \lesssim z \lesssim 4 \text{ kpc}$ (Kordopatis et al. 2011), we conclude that all stars from our sample probably belong to the Galactic halo.

4. Search for nebular lines and infrared excess

All of our five stars are located in the region of CSPNe in the $\log T_{\text{eff}} - \log g$ diagram, which suggests that they might be central stars as well. The large distances of the stars, however, imply rather small angular diameters of the order of one arcsec or even less (assuming a typical expansion velocity of 20 km/s and distances and post-AGB times from Table 3). Thus, it is unlikely to detect PNe around these stars via ground-based imaging. Therefore, it is much more promising to search for prominent nebular emission lines in the spectra of these stars, i.e., the $[\text{O III}] \lambda\lambda 4959, 5007 \text{ \AA}$ emission lines, which are typically the strongest lines for a medium to high-excitation PN. Because of the long exposure times and the much better background subtraction that can be achieved in slit or fibre spectroscopy compared to narrow-band imaging or slitless objective prism imaging spectroscopy, SDSS spectra allow the detection of extremely faint PN (down to

29–30 mag arcsec⁻¹, Yuan & Liu 2013). However, we could not detect any hint for nebular lines in the spectra of our five stars.

The detection of an infrared (IR) excess can put constraints on the nature of a possible companion, or the presence of a circumstellar disk. To search for possible IR excess emission around our five stars, we cross matched their positions with the UKIDSS (UKIRT Infrared Deep Sky Survey) DR9 catalog (Lawrence et al. 2013) and the WISE (Wide-field Infrared Survey Explorer) catalog (Cutri & et al. 2014). We applied a search radius of 2 arcsec. For the O(H) stars J0935 and J2046 no IR colors were found, but for J1000 and the PG 1159 star J1556 we found *J* and *H* entries. For the O(He) star J0757 we found a *J* value. The PG 1159 star J1556 is the only object with entries in the WISE catalog. In addition, GALEX *FUV* and *NUV* (Bianchi et al. 2014) and SDSS magnitudes (Ahn et al. 2012) were obtained for all objects. Magnitudes and reddening of the five stars are summarized in Table 2. SDSS, UKIDSS, and WISE magnitudes were converted into fluxes as outlined in Verbeek et al. (2014). For the GALEX magnitudes conversions³, we used

$$f_{\text{FUV}} [\text{erg s}^{-1} \text{cm}^{-2} \text{\AA}^{-1}] = 1.40 \times 10^{-15} 10^{-0.4 (FUV-18.82)}$$

$$f_{\text{NUV}} [\text{erg s}^{-1} \text{cm}^{-2} \text{\AA}^{-1}] = 2.06 \times 10^{-16} 10^{-0.4 (NUV-20.08)}.$$

Then, we corrected the TMAP model flux of our best fit for each star for interstellar reddening using the reddening law of Fitzpatrick (1999). Again, we used the values for E_{B-V} from the Galactic dust extinction maps of Schlafly & Finkbeiner (2011). Thereafter, we normalized the reddened model flux to the SDSS *g* magnitude and checked if the other color measurements are within 3σ in agreement with the model fluxes.

A perfect agreement with the color measurements and the reddened model flux was found for the three O(H) stars and the O(He) star, i.e. no evidence for an excess was found in the near IR. The PG 1159 star J1556, however, displays a clear excess in all WISE colors (Fig. 6). Due to the lack of WISE measurements a search for an far-IR excess was not possible for the other four stars. In the (W2–W3), (W3–W4) diagram, the WISE colors of J1556 agree with the bulk of PNe (Kronberger et al. 2014). However, as mentioned above, no nebular emission lines are visible in the SDSS spectrum (total exposure time ≈ 2.25 h).

An IR excess that strongly shows up in the Spitzer IRAC bands (Xu & Jura 2012), was found around some warm (i.e., $T_{\text{eff}} \leq 25\,000$ K) white dwarfs. This IR excess is interpreted as originating from a small hot disk due to the infall and destruction of single asteroids that come within the star’s Roche limit (Gänsicke et al. 2006). However, we exclude the presence of a debris disk in the case of J1556, because at such high T_{eff} , solids would be sublimated into gaseous disks (von Hippel et al. 2007). In addition the double-peaked Ca II triplet, which is the hallmark of a gaseous, rotating disk (Young et al. 1981; Horne & Marsh 1986), cannot be detected.

Cold dust disks, which are located much farther from the star (≈ 50 AU compared to ≤ 0.01 AU for the debris disks) have been announced for a number of hot white dwarfs and CSPNe and are likely formed by mass loss from the stars during their AGB phase (Clayton et al. 2014; Chu et al. 2011). These disks, however, were found to be relatively cool (≈ 100 K compared ≈ 1000 K for the debris disks) and should show up only in the W4 band. The relatively flat IR excess in J1556 cannot be fitted with a single blackbody and looks very similar like in the case of the CSPN K 1-22. Chu et al. (2011) showed that for K 1-22,

the IR excess is a superposition of the photospheric emission of the CSPN and a red companion as well as the dust continuum. Thus, it is likely that more than one source contributes to the IR excess of J1556 as well.

Finally, we note that the IR excess could also have an extragalactic origin. We corrected the WISE colors of J1556 for the stellar flux contribution and obtained $W1 = 18.40$, $W2 = 16.54$, $W3 = 12.23$, and $W4 = 8.93$. This leads to $W1-W2 = 1.86$ and $W2-W3 = 4.31$, which corresponds to the region of luminous IR galaxies or Sbc star-burst galaxies in the (W1–W2), (W2–W3) diagram (Fig. 12 in Wright et al. 2010). The WISE-excess might therefore be caused by a chance alignment of such a background galaxy with J1556. However, the probability for such an alignment of two very peculiar classes of objects seems to be very unlikely.

5. Discussion

The high RV variations - partly on short time scales - detected in four of our stars are a strong hint that they are part of close binary systems. Unlike hot subdwarfs, which are expected to have lost almost their entire envelope already on the RGB via stable Roche lobe overflow and/or common envelope evolution, the mass-loss on the RGB of post-AGB close binaries must have been weaker. This is because only stars with an sufficiently thick envelope are able to maintain H-shell burning and to ascend the AGB.

The post-AGB phase (i.e., the evolution from the AGB towards the maximum T_{eff}) is very short-lived. The evolutionary time scales depend strongly on the stellar mass, so that a $0.53 M_{\odot}$ star needs about 80 000 yr to reach its maximum T_{eff} , while a $0.83 M_{\odot}$ stars reaches its maximum T_{eff} within less than 1000 yrs (Miller Bertolami 2015). It is expected that each post-AGB star eventually becomes a CSPN, if the star is able to ionize the previously ejected outer layers before the expanding envelope becomes too tenuous to appear as a PN.

As mentioned above all of our five stars are located in the $\log T_{\text{eff}} - \log g$ diagram just amongst the CSPNe. However, no nebular lines can be detected in their spectra. We will therefore discuss in the following the evolutionary status of these objects taking into account the absence of a PN around these stars as well as their possible close binary nature.

5.1. The PG 1159 star J1556

The phenomenon of the “missing” PN is well known for the H-deficient PG 1159 and O(He) stars. Only 15 of the 47 currently known PG 1159 stars are confirmed CSPNe, which can be understood with regard to their evolutionary history. PG 1159 stars are believed to be the result of a (V)LTP that occurs either during the blueward excursion of the post-AGB star (LTP), or during its early white dwarf cooling phase (VLTP). The release of nuclear energy by the flashing helium shell forces the already very compact star to expand back to giant dimensions - the so-called born-again scenario (Fujimoto 1977; Schönberner 1979; Iben et al. 1983; Althaus et al. 2005). The absence of hydrogen in the atmosphere of J1556 combined with the appearance of N V lines in the SDSS spectrum suggests a VLTP (Werner & Herwig 2006). Since for He-burners a three times longer evolutionary time scale is predicted (Iben et al. 1983) and given that J1556 is going through the post-AGB phase for the second time, the “missing” PN can be understood very well.

Should the RV variations in J1556 be confirmed to originate from a close companion, then J1556 would be just

³ http://asd.gsfc.nasa.gov/archive/galex/FAQ/counts_background.html

the second known PG 1159 close binary system besides SDSS J212531.92–010745.9 (Nagel et al. 2006; Schuh et al. 2009; Shimansky et al. 2015). The companion in the latter system is a low mass main sequence star as it is obvious from the reflection effect in the light curve and from the Hydrogen Balmer series which appears in emission due to the radiation of the PG 1159 star (Nagel et al. 2006). However, in the spectra of J1556, we cannot find evidence for such emission lines. The IR excess of J1556 shows up only in the WISE bands, which suggest that a possible companion to J1556 might be even less massive. We stress that SDSS J212531.92–010745.9 is at least two orders of magnitude less luminous compared to J1556, and thus it is much more difficult to detect a low mass main sequence star for the latter.

Amongst the H-deficient Wolf Rayet type central stars, which are believed to be the progenitors of the PG 1159 stars (Werner & Herwig 2006), only three close binary systems have been discovered so far (Hajduk et al. 2010; Manick et al. 2015). This leads to a known close binary fraction of about 5% amongst these C-dominated objects⁴, which is significantly less compared to the overall close binary fraction of CSPNe ($\approx 15 - 20\%$, Bond 2000; Miszalski et al. 2009). This suggests, that binary interaction may not play a fundamental role in forming C-dominated stars. Definitive statements can, however, only be made after a systematic search of close binaries amongst these stars.

5.2. The O(He) star J0757

J0757 is the first RV variable O(He) star ever discovered. De Marco et al. (2015) recently discovered the O(He)-type CSPN of Pa 5 (PN G076.3+14.1) to have a consistent photometric period of 1.12 d in twelve individual Kepler quarters. However, they failed to detect RV shifts larger than 5 km/s. They argue, that the photometric variability may be explained by the influence of an orbiting planet or magnetic activity, but most likely by a evolved companion in a nearly-pole-on orbit. Given that there are currently only ten O(He) stars known, the confirmation of close binaries to J0757 and Pa 5 would already indicate a binary fraction of 20%. This may suggest, that close binary evolution is, at least for some of the He-dominated objects, an important formation channel.

Also amongst He-dominated stars, a PN seems to be the exception rather than the rule. In addition, it appears that the presence of a PN is restricted to N-rich O(He) stars and [WN]-type CSPNe only, which suggests that these objects are formed differently than C-rich or C+N-rich He-dominated objects (Reindl et al. 2014b). The possibility that the latter two subclasses are formed via the merger of two white dwarfs naturally explains the missing PN, because of the very long predicted post-merger times of the stars. Though, the confirmation of a close companion to J0757 would question the merger scenario as triple star systems are arranged hierarchically. Moreover, it is questionable if it is possible that unstable mass transfer could stop before the merger of two white dwarfs is complete, and thus leaving behind a very low mass close companion (Justham et al. 2010; Han & Webbink 1999).

We consider therefore yet another possibility to explain both, the “missing” PN as well as the extreme maximum RV shift of 107.0 ± 22.0 km/s within only 31 min (which is already pointing toward a very close binary system), namely that J0757 could have evolved from an AMCVn type system which stopped ac-

cretion. AMCVn stars are He transferring ultracompact binary systems with orbital period below 1 h. The mass ratio of these systems is expected to be sufficiently low and therefore, stable mass transfer occurs. These systems prevent the merger and with decreasing accretion rates, they evolve towards longer orbital periods (Yungelson et al. 2002; Marsh et al. 2004; Nelemans et al. 2010). The accretors of these systems may experience stable He-burning (Piersanti et al. 2014, 2015). In case the progenitor of J0757 was a He WD, which ignited He-burning, the post accretion evolution might look similar as in the case of the post-double He white dwarf merger models of Zhang & Jeffery (2012a,b) and, thus, would imply that J0757 must have evolved through the region of the central He burning He-sdO stars (lower panel of Fig. 5).

Quite interestingly, we find that the great majority (up to 84%) of the RV variable He-sdO stars discovered by Geier et al. (2015), belong to the class of C-rich He-dominated objects⁵ just like J0757. Also note that the irregular RV variations detected by Geier et al. (2015) in some of the He-sdO stars (e.g., the C-rich He-sdO SDSS J232757.46+483755.2), might even support this scenario, if we assume that they are caused by a still present accretion stream (Schwarz et al. 2010).

5.3. H-rich stars

J1000 and J0935 are the first RV variable naked O(H) stars ever discovered. So far, only five other naked O(H) stars are known: BD+18 2647 (Bauer & Husfeld 1995), ROB 162 in the globular cluster NGC 6397 (Heber & Kudritzki 1986), vZ1128 in the globular cluster M 3 (Chayer et al. 2015), GD 605, which is also considered as halo star (Fontaine et al. 2008), as well as the metal poor O(H) star LS IV-12 1 (Heber & Hunger 1987). The fact that no PN is present around these stars is rather unexpected, since in our canonical understanding each star that evolves through the AGB is expected to produce a PN. A simple explanation for their “missing” PNe could be that their post-AGB times are longer than the time it took for the PNe to disappear into the interstellar medium. This possibility is, however, put into doubt, when we have a look in Fig. 3, where we show in addition to the eight known naked O(H) stars also the locations of H-rich CSPNe found in the literature. We derived the post-AGB times from the post-AGB tracks of Miller Bertolami (2015) for the seven naked O(H) stars as well as the H-rich CSPNe. As it can be seen from Table 3, we found that - compared to the eight naked O(H) stars - there are several CSPNe with apparently much longer post-AGB times⁶.

On that basis, it is obscure why those stars still harbor a PNe, but not the seven naked O(H) stars and it raises the question: Does every post-AGB star, and in particular also every close binary post-AGB system, necessarily produce a PNe? This would be particularly important to understand in view of the proposed role of close binary post-AGB stars in the formation of asymmetrical PNe. We stress that if J1000 and J0935 indeed turn out to be close binary systems, this would lead to a close binary

⁵ Classification based on the presence of C lines, but absence of N lines in the SDSS spectra. The remaining RV variable He-sdO stars either do not show any metal lines (8%) or belong to the group of C+N-rich He-sdO stars (8–12%).

⁶ Note that for the two DA white dwarf CSPNe HaWe 5 and HDW 4, Napiwotzki (1999) even found post-AGB times of several million years, which, however, strongly contradicted the very short kinematical ages of both PNe (less than 4 kyr). Napiwotzki (1999) suggested that PNe of these stars might actually be ejected nova shells.

⁴ There are currently about 60 Wolf Rayet type central stars known (H.Todt, priv. comm.).

Table 3. Post-AGB times as derived from H-burning post AGB tracks of Miller Bertolami (2015) of the eight naked O(H) stars and some CSPNe with very long post-AGB times. For objects that are not covered by these tracks, we give lower limits.

	name	$t_{\text{post-AGB}}$
	LS IV-12 1 ^(a)	9 kyr
	GD 605 ^(b)	20 kyr
	J2046 ^(c)	31 kyr
	J0935 ^(c)	31 kyr
	J1000 ^(c)	33 kyr
	vZ1128 ^(d)	38 kyr
	ROB 162 ^(e)	49 kyr
	BD+18 2647 ^(f)	56 kyr
PN G	name	$t_{\text{post-AGB}}$
047.0+42.4	A 39 ^(g)	73 kyr
072.7-17.1	A 74 ^(h)	80 kyr
158.9+17.8	PuWe 1 ^(h)	80 kyr
025.4-04.7	IC 1295 ^(h)	> 80 kyr
030.6+06.2	Sh 2-68 ^(h)	> 80 kyr
158.5+00.7	Sh 2-216 ⁽ⁱ⁾	> 80 kyr
077.6+14.7	A 61 ^(g)	90 kyr
128.0-04.1	Sh 2-188 ⁽ⁱ⁾	120 kyr
047.0+42.4	A 39 ^(f)	73 kyr
072.7-17.1	A 74 ^(g)	80 kyr
158.9+17.8	PuWe 1 ^(f)	80 kyr
025.4-04.7	IC 1295 ^(g)	> 80 kyr
030.6+06.2	Sh 2-68 ^(g)	> 80 kyr
158.5+00.7	Sh 2-216 ^(h)	> 80 kyr
077.6+14.7	A 61 ^(f)	90 kyr
128.0-04.1	Sh 2-188 ⁽ⁱ⁾	120 kyr

Notes. Post-AGB times derived from atmospheric parameters, which were taken from ^(a) Heber & Hunger (1987), ^(b) Fontaine et al. (2008), ^(c) this work, ^(d) Chayer et al. (2015), ^(e) Heber & Kudritzki (1986), ^(f) Bauer & Husfeld (1995), ^(g) Napiwotzki (1999), ^(h) Ziegler (2012), ⁽ⁱ⁾ Rauch et al. (2007), ^(j) Gianninas et al. (2010),

fraction of 25% amongst naked O(H) stars, which is even higher than what is found for the CSPNe.

An alternative solution to the non-ejection of a PNe of apparently naked O(H) stars was suggested by Heber & Hunger (1987), namely that also these stars suffered a LTP. Contrary to the VLTP scenario, which always results in a H-deficient surface composition since H is mixed and burnt already during the thermal pulse, the LTP does not necessarily predict a H-poor star. This is because in the case of a LTP, the convective shell triggered by excessive He burning is not able to penetrate the H-rich envelope from below because the entropy jump across the He/H interface is too large. Only when the star evolves back to its Hayashi limit on the AGB ($T_{\text{eff}} \lesssim 7000$ K), envelope convection sets in again (Blöcker & Schönberner 1996, 1997; Schönberner 2008). Evolutionary calculations without overshoot (e.g., Blöcker & Schönberner 1997) predict only mild, if any, mixing. The envelope convection does not reach the layers enriched with carbon, and no third dredge up occurs. Later calculations by Herwig (2001) showed that if overshoot is applied to all convective regions, AGB models show efficient dredge up even for very low envelope masses and thus produce H-deficient stars. Observational proof for the validity of the latter case is offered by FG Sge, the only star known to this day that certainly

must have suffered a LTP (Schönberner 2008). This star was actually observed evolving back to the AGB were the H fraction in its atmosphere got diluted significantly (from 0.9 to 0.01, by number, Jeffery & Schönberner 2006).

Finally, it is interesting to note that there are also some F or G type supergiants which have already departed from the AGB, but lack a reflection nebula, and as such are not expected to evolve into a CSPN. These much cooler objects (compared to the O(H) stars discussed above) show the presence of a compact disk with an inner radius of ≈ 15 AU (Deroo et al. 2006, 2007) and in addition they were found to reside in binary systems. They have orbital periods between a hundred and a couple of thousands days, and probably unevolved (very) low initial mass companions (van Winckel et al. 2009). It is thought, that these stars probably did have a pre-PN before, but that the re-accretion of material has stalled the blue-ward evolution of the post-AGB star and, thus, providing the circumstellar material enough time to disperse before it cloud became ionized (De Marco 2014).

6. Conclusions

Our non-LTE model atmosphere analysis revealed that all five stars, which were recently discovered by the MUCHFUSS project as RV stars, lie in the post-AGB region of the HRD. The RV variations were found not to be significant in case of the O(H) star J2046, but in the cases of the other two O(H) stars (J1000, J0935), the O(He) star (J0757), and the PG 1159 star (J1556). This reveals J0757 as the first RV variable O(He) star ever discovered, J1556 as the only second known RV variable PG 1159 star, and J1000 and J0935 as the first RV variable O(H) stars that do not show any hint of a PN.

The absence of a PN around the PG 1159 star J1556 can be explained well in terms of a VLTP evolution, which can also account for the high C abundance. Given the currently known low binary fraction of C-dominated stars, it appears at the moment that binary interactions do not play a crucial role in the formation of these stars.

In case of the O(He) star J0757 we speculate that it once was part of a compact He transferring binary systems in which the mass transfer had stop after a certain time, leaving behind a low mass close companion. In this way one could explain both, the absence of a PN as well as the RV shift of 107.0 ± 22.0 km/s measured within only 31 min. Surely, these speculations need more observational as well as theoretical support, however, they might offer a yet not considered evolutionary channel for the mysterious He-dominated objects.

Various explanations could hold for the “missing” PNe around the O(H)-type stars. The possibility that the post-AGB times of the naked O(H) stars are longer than it took for the PNe to disappear into the interstellar medium, seems odd given the fact that there are several CSPNe with much longer post-AGB times. Besides the non-ejection of a PN, the occurrence of a LTP, or the re-accretion of the PN in the previous post-AGB evolution offer possible explanations for those stars not harbouring a PN (any more).

The search for an IR excess was successful only in the case of J1556, which displays a clear IR excess in all WISE colors. In order to understand its nature, spectroscopic follow-up observations are necessary. We should, however, keep in mind that it is very difficult to detect a close companion via the IR excess method given the very high luminosities of stars in post-AGB region (our stars have several thousand times the solar luminosity, Table 1). Thus, the presence of a late type companion to the other stars in our sample cannot be excluded from the outset.

Acknowledgements. N.R. was supported by DFG (grant WE1312/41-1) and DLR (grant 50 OR 1507). We thank Marcelo Miguel Miller Bertolami for providing us with the post-AGB tracks before they were published. We thank Thomas Rauch and Peter van Hoof for helpful discussions and comments. Based on observations collected at the Centro Astronómico Hispano Alemán (CAHA) at Calar Alto, operated jointly by the Max-Planck Institut für Astronomie and the Instituto de Astrofísica de Andalucía (CSIC). Based on observations with the William Herschel and Isaac Newton Telescopes operated by the Isaac Newton Group at the Observatorio del Roque de los Muchachos of the Instituto de Astrofísica de Canarias on the island of La Palma, Spain. Funding for SDSS-III has been provided by the Alfred P. Sloan Foundation, the Participating Institutions, the National Science Foundation, and the U.S. Department of Energy Office of Science. The SDSS-III web site is <http://www.sdss3.org/>. SDSS-III is managed by the Astrophysical Research Consortium for the Participating Institutions of the SDSS-III Collaboration including the University of Arizona, the Brazilian Participation Group, Brookhaven National Laboratory, Carnegie Mellon University, University of Florida, the French Participation Group, the German Participation Group, Harvard University, the Instituto de Astrofísica de Canarias, the Michigan State/Notre Dame/JINA Participation Group, Johns Hopkins University, Lawrence Berkeley National Laboratory, Max Planck Institute for Astrophysics, Max Planck Institute for Extraterrestrial Physics, New Mexico State University, New York University, Ohio State University, Pennsylvania State University, University of Portsmouth, Princeton University, the Spanish Participation Group, University of Tokyo, University of Utah, Vanderbilt University, University of Virginia, University of Washington, and Yale University. This research has made use of the VizieR catalogue access tool, CDS, Strasbourg, France.

References

- Ahn, C. P., Alexandroff, R., Allende Prieto, C., et al. 2012, *ApJS*, 203, 21
 Althaus, L. G., Serenelli, A. M., Panei, J. A., et al. 2005, *A&A*, 435, 631
 Asplund, M., Grevesse, N., Sauval, A. J., & Scott, P. 2009, *ARA&A*, 47, 481
 Barnard, A. J., Cooper, J., & Shamey, L. J. 1969, *A&A*, 1, 28
 Barnard, A. J., Cooper, J., & Smith, E. W. 1974, *J. Quant. Spec. Radiat. Transf.*, 14, 1025
 Bauer, F. & Husfeld, D. 1995, *A&A*, 300, 481
 Bianchi, L., Conti, A., & Shiao, B. 2014, *VizieR Online Data Catalog*, 2335, 0
 Blöcker, T. & Schönberner, D. 1996, *Mem. Soc. Astron. Italiana*, 67, 665
 Blöcker, T. & Schönberner, D. 1997, *A&A*, 324, 991
 Bond, H. E. 2000, in *Astronomical Society of the Pacific Conference Series*, Vol. 199, *Asymmetrical Planetary Nebulae II: From Origins to Microstructures*, ed. J. H. Kastner, N. Soker, & S. Rappaport, 115
 Brown, T. M., Sweigart, A. V., Lanz, T., Landsman, W. B., & Hubeny, I. 2001, *ApJ*, 562, 368
 Chayer, P., Dixon, W. V., Fullerton, A. W., Ooghe-Tabanou, B., & Reid, I. N. 2015, *MNRAS*, 452, 2292
 Chu, Y.-H., Su, K. Y. L., Bilikova, J., et al. 2011, *AJ*, 142, 75
 Clayton, G. C., De Marco, O., Nordhaus, J., et al. 2014, *AJ*, 147, 142
 Cutri, R. M. & et al. 2014, *VizieR Online Data Catalog*, 2328, 0
 De Marco, O. 2014, in *Asymmetrical Planetary Nebulae VI Conference*, 122
 De Marco, O., Farihi, J., & Nordhaus, J. 2009, *Journal of Physics Conference Series*, 172, 012031
 De Marco, O., Hillwig, T. C., & Smith, A. J. 2008, *AJ*, 136, 323
 De Marco, O., Long, J., Jacoby, G. H., et al. 2015, *MNRAS*, 448, 3587
 Deroo, P., Acke, B., Verhoelst, T., et al. 2007, *A&A*, 474, L45
 Deroo, P., van Winckel, H., Min, M., et al. 2006, *A&A*, 450, 181
 Dimitrijević, M. S. & Sahal-Brechot, S. 1992, *A&AS*, 96, 613
 Dimitrijević, M. S., Sahal-Brechot, S., & Bommier, V. 1991, *Bulletin de l'Observatoire Astronomique de Belgrade*, 144, 65
 Dreizler, S. & Werner, K. 1996, *A&A*, 314, 217
 Fitzpatrick, E. L. 1999, *PASP*, 111, 63
 Fontaine, M., Chayer, P., Oliveira, C. M., Wesemael, F., & Fontaine, G. 2008, *ApJ*, 678, 394
 Fujimoto, M. Y. 1977, *PASJ*, 29, 331
 Gänsicke, B. T., Marsh, T. R., Southworth, J., & Rebassa-Mansergas, A. 2006, *Science*, 314, 1908
 Geier, S., Hirsch, H., Tillich, A., et al. 2011, *A&A*, 530, A28
 Geier, S., Kupfer, T., Heber, U., et al. 2015, *A&A*, 577, A26
 Gianninas, A., Bergeron, P., Dupuis, J., & Ruiz, M. T. 2010, *ApJ*, 720, 581
 Griem, H. R. 1974, *Spectral line broadening by plasmas* (New York, Academic Press, Inc. Pure and Applied Physics. Volume 39, 1974. 421)
 Hajduk, M., Zijlstra, A. A., & Gesicki, K. 2010, *MNRAS*, 406, 626
 Han, Z. & Webbink, R. F. 1999, *A&A*, 349, L17
 Heber, U. & Hunger, K. 1987, *The Messenger*, 47, 36
 Heber, U., Hunger, K., Jonas, G., & Kudritzki, R. P. 1984, *A&A*, 130, 119
 Heber, U. & Kudritzki, R. P. 1986, *A&A*, 169, 244
 Herald, J. E. & Bianchi, L. 2011, *MNRAS*, 417, 2440
 Herwig, F. 2001, in *Astrophysics and Space Science Library*, Vol. 265, *Astrophysics and Space Science Library*, ed. R. Szczerba & S. K. Górný, 249
 Hirsch, H. A. 2009, PhD thesis, University Erlangen-Nürnberg
 Horne, K. & Marsh, T. R. 1986, *MNRAS*, 218, 761
 Hügelmeier, S. D., Dreizler, S., Homeier, D., et al. 2006, *A&A*, 454, 617
 Iben, Jr., I., Kaler, J. B., Truran, J. W., & Renzini, A. 1983, *ApJ*, 264, 605
 Iben, Jr., I. & Tutukov, A. V. 1984, *ApJS*, 54, 335
 Iben, Jr., I. & Tutukov, A. V. 1986, *ApJ*, 311, 742
 Jeffery, C. S. & Schönberner, D. 2006, *A&A*, 459, 885
 Justham, S., Podsiadlowski, P., & Han, Z. 2011, *MNRAS*, 410, 984
 Justham, S., Podsiadlowski, P., Han, Z., & Wolf, C. 2010, *Ap&SS*, 329, 3
 Kalirai, J. S. 2012, *Nature*, 486, 90
 Kordopatis, G., Recio-Blanco, A., de Laverny, P., et al. 2011, *A&A*, 535, A107
 Kronberger, M., Jacoby, G. H., Harmer, D., & Patchick, D. 2014, in *Asymmetrical Planetary Nebulae VI Conference*, 47
 Lanz, T., Brown, T. M., Sweigart, A. V., Hubeny, I., & Landsman, W. B. 2004, *ApJ*, 602, 342
 Latour, M., Fontaine, G., Brassard, P., Chayer, P., & Green, E. M. 2010, in *American Institute of Physics Conference Series*, Vol. 1273, *American Institute of Physics Conference Series*, ed. K. Werner & T. Rauch, 255–258
 Latour, M., Fontaine, G., Green, E. M., & Brassard, P. 2015, *A&A*, 579, A39
 Lawrence, A., Warren, S. J., Almaini, O., et al. 2013, *VizieR Online Data Catalog*, 2319, 0
 Lemke, M. 1997, *A&AS*, 122, 285
 Mahserici, M. 2011, Diploma thesis, University Tübingen, Germany
 Manick, R., Miszalski, B., & McBride, V. 2015, *MNRAS*, 448, 1789
 Marsh, T. R., Nelemans, G., & Steeghs, D. 2004, *MNRAS*, 350, 113
 Maxted, P. F. L., Heber, U., Marsh, T. R., & North, R. C. 2001, *MNRAS*, 326, 1391
 Mendez, R. H. 1991, in *IAU Symposium*, Vol. 145, *Evolution of Stars: the Photospheric Abundance Connection*, ed. G. Michaud & A. V. Tutukov, 375
 Miller Bertolami, M. M. 2015, *ArXiv e-print* 1512.04129
 Miller Bertolami, M. M. & Althaus, L. G. 2006, *A&A*, 454, 845
 Miller Bertolami, M. M. & Althaus, L. G. 2007, *A&A*, 470, 675
 Miszalski, B., Acker, A., Moffat, A. F. J., Parker, Q. A., & Udalski, A. 2009, *A&A*, 496, 813
 Nagel, T., Schuh, S., Kusterer, D.-J., et al. 2006, *A&A*, 448, L25
 Napiwotzki, R. 1999, *A&A*, 350, 101
 Napiwotzki, R., Yungelson, L., Nelemans, G., et al. 2004, in *Astronomical Society of the Pacific Conference Series*, Vol. 318, *Spectroscopically and Spatially Resolving the Components of the Close Binary Stars*, ed. R. W. Hilditch, H. Hensberge, & K. Pavlovski, 402–410
 Nelemans, G., Yungelson, L. R., van der Sluys, M. V., & Tout, C. A. 2010, *MNRAS*, 401, 1347
 Paczynski, B. 1976, in *IAU Symposium*, Vol. 73, *Structure and Evolution of Close Binary Systems*, ed. P. Eggleton, S. Mitton, & J. Whelan, 75
 Parker, Q. A., Acker, A., Frew, D. J., et al. 2006, *MNRAS*, 373, 79
 Piersantí, L., Tornambé, A., & Yungelson, L. R. 2014, *MNRAS*, 445, 3239
 Piersantí, L., Yungelson, L. R., & Tornambé, A. 2015, *MNRAS*, 452, 2897
 Rauch, T. & Deetjen, J. L. 2003, in *Astronomical Society of the Pacific Conference Series*, Vol. 288, *Stellar Atmosphere Modeling*, ed. I. Hubeny, D. Mihaslas, & K. Werner, 103
 Rauch, T., Köppen, J., & Werner, K. 1994, *A&A*, 286, 543
 Rauch, T., Ziegler, M., Werner, K., et al. 2007, *A&A*, 470, 317
 Reindl, N., Rauch, T., Werner, K., et al. 2014a, *A&A*, 572, A117
 Reindl, N., Rauch, T., Werner, K., Kruk, J. W., & Todt, H. 2014b, *A&A*, 566, A116
 Schlafly, E. F. & Finkbeiner, D. P. 2011, *ApJ*, 737, 103
 Schönberner, D. 1979, *A&A*, 79, 108
 Schönberner, D. 2008, in *Astronomical Society of the Pacific Conference Series*, Vol. 391, *Hydrogen-Deficient Stars*, ed. A. Werner & T. Rauch, 139
 Schöning, T. & Butler, K. 1989, *A&AS*, 78, 51
 Schuh, S., Beeck, B., & Nagel, T. 2009, *Journal of Physics Conference Series*, 172, 012065
 Schwarz, C., Montgomery, M. M., & Martin, E. L. 2010, in *American Institute of Physics Conference Series*, Vol. 1273, *American Institute of Physics Conference Series*, ed. K. Werner & T. Rauch, 362–365
 Shimansky, V. V., Borisov, N. V., Nurtidnova, D. N., et al. 2015, *Astronomy Reports*, 59, 199
 Stroeger, A., Heber, U., Lisker, T., et al. 2007, *A&A*, 462, 269
 Tremblay, P.-E. & Bergeron, P. 2009, *ApJ*, 696, 1755
 van Winckel, H., Lloyd Evans, T., Briquet, M., et al. 2009, *A&A*, 505, 1221
 Verbeek, K., Groot, P. J., Scaringi, S., et al. 2014, *MNRAS*, 438, 2
 von Hippel, T., Kuchner, M. J., Kilic, M., Mullally, F., & Reach, W. T. 2007, *ApJ*, 662, 544
 Wassermann, D., Werner, K., Rauch, T., & Kruk, J. W. 2010, *A&A*, 524, A9
 Webbink, R. F. 1984, *ApJ*, 277, 355

Werner, K., Deetjen, J. L., Dreizler, S., et al. 2003, in *Astronomical Society of the Pacific Conference Series*, Vol. 288, *Stellar Atmosphere Modeling*, ed. I. Hubeny, D. Mihalas, & K. Werner, 31

Werner, K. & Herwig, F. 2006, *PASP*, 118, 183

Werner, K. & Rauch, T. 2014, *A&A*, 569, A99

Werner, K., Rauch, T., & Kepler, S. O. 2014, *A&A*, 564, A53

Wright, E. L., Eisenhardt, P. R. M., Mainzer, A. K., et al. 2010, *AJ*, 140, 1868

Xu, S. & Jura, M. 2012, *ApJ*, 745, 88

Young, P., Schneider, D. P., & Sackett, S. A. 1981, *ApJ*, 245, 1035

Yuan, H. B. & Liu, X. W. 2013, *MNRAS*, 436, 718

Yungelson, L. R., Nelemans, G., & van den Heuvel, E. P. J. 2002, *A&A*, 388, 546

Zhang, X. & Jeffery, C. S. 2012a, *MNRAS*, 426, L81

Zhang, X. & Jeffery, C. S. 2012b, *MNRAS*, 419, 452

Zhang, X., Jeffery, C. S., Chen, X., & Han, Z. 2014, *MNRAS*, 445, 660

Ziegler, M. 2012, Dissertation, University of Tübingen, Germany, <https://publikationen.uni-tuebingen.de/xmlui/handle/10900/50006>

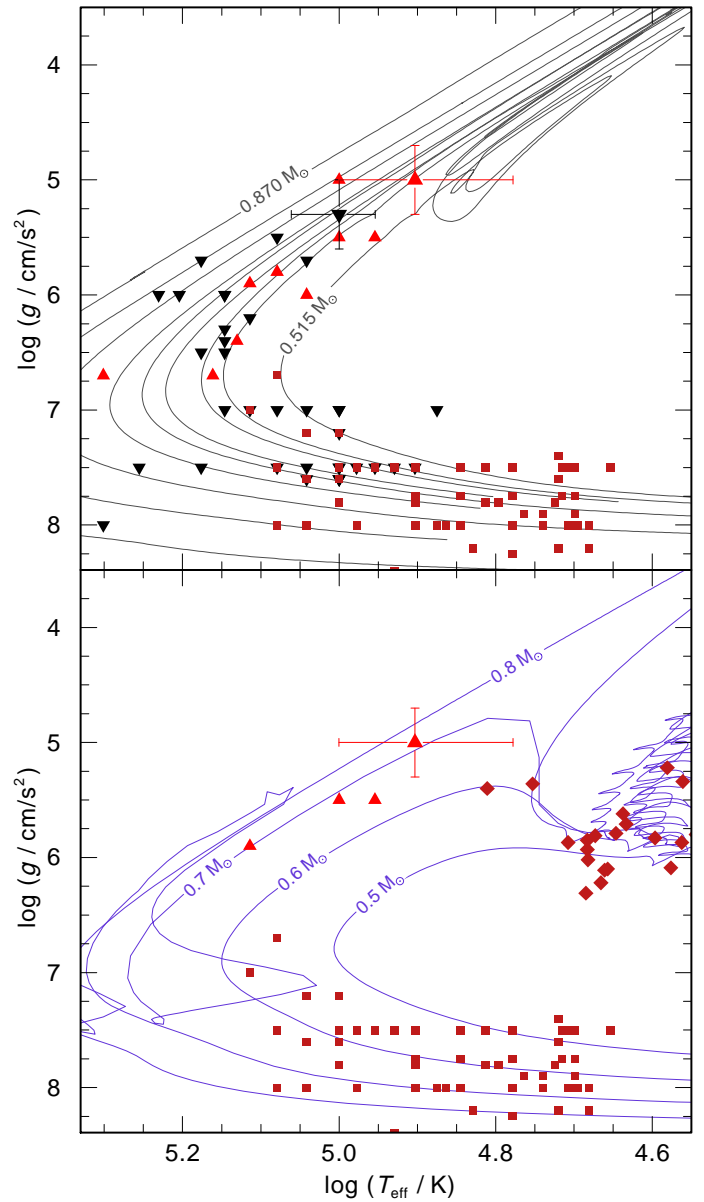


Fig. 5. Locations of the O(He) star J0757 (red triangle with error bars) and the PG 1159 star J1556 (black inverted triangle with error bars) and other PG 1159 and O(He) stars (black inverted triangles and red triangles, respectively, De Marco et al. 2015; Reindl et al. 2014b; Werner & Rauch 2014; Werner et al. 2014; Gianninas et al. 2010; Wassermann et al. 2010; Werner & Herwig 2006) in the $T_{\text{eff}} - \log g$ diagram. Their likely successors, the H-deficient white dwarfs (Reindl et al. 2014a; Werner et al. 2014; Mahsereci 2011; Hügelmeyer et al. 2006; Dreizler & Werner 1996) are indicated by filled, red squares. The *upper panel* compares the location of these stars to (V)LTP evolutionary tracks (grey lines) of Miller Bertolami & Althaus (2007, 2006). For clarity, only two tracks are labeled with stellar masses. Intermediate tracks correspond to 0.530, 0.542, 0.565, 0.584, 0.609, 0.664, 0.741 M_{\odot} . The *lower panel* compares only the locations of the C-rich O(He) stars (red triangles) and C-strong lined He-sdO stars (red rhombs) from the sample of Geier et al. (2015) with post-double He white dwarf merger tracks (purple lines) of Zhang & Jeffery (2012a,b).

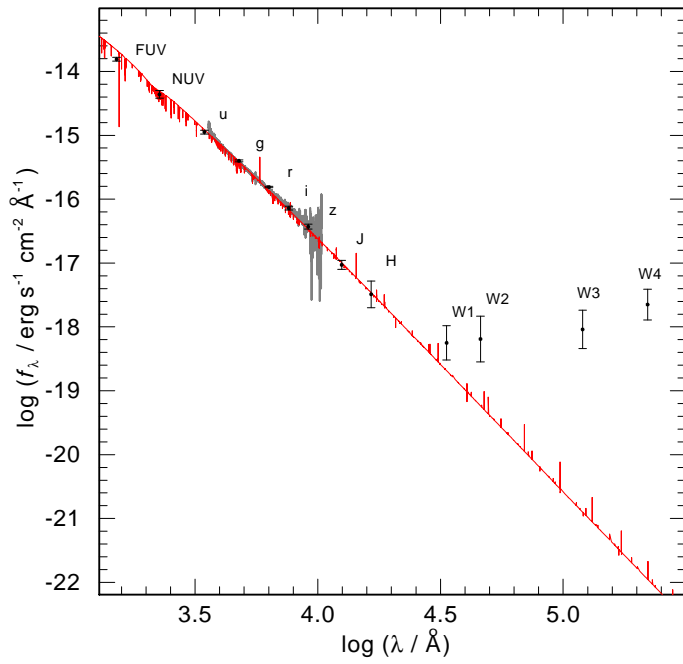


Fig. 6. Colors (black dots with 3σ error bars) and the SDSS spectrum (grey) of the PG 1159 star J1556 (grey), compared with a reddened TMAP model SED (black, red in online version). The emission lines are of photospheric origin. Note that the mismatch of the reddened model flux and the GALEX *FUV* measurement is due to missing metal opacities in our model atmosphere.

Table 2. Magnitudes and reddening of the stars

Object	J0935	J1000	J2046	J1556	J0757
E_{B-V}	0.018 ± 0.001	0.036 ± 0.002	0.058 ± 0.003	0.058 ± 0.005	0.030 ± 0.001
FUV	16.325 ± 0.019	15.799 ± 0.019	15.993 ± 0.034	16.157 ± 0.036	16.755 ± 0.037
NUV	16.899 ± 0.015	16.431 ± 0.016	16.555 ± 0.031	16.712 ± 0.018	17.297 ± 0.033
u	17.672 ± 0.010	17.053 ± 0.007	17.075 ± 0.008	17.241 ± 0.009	17.837 ± 0.012
g	18.114 ± 0.006	17.483 ± 0.005	17.450 ± 0.005	17.675 ± 0.006	18.280 ± 0.007
r	18.681 ± 0.009	18.019 ± 0.007	17.884 ± 0.007	18.141 ± 0.007	18.775 ± 0.010
i	19.075 ± 0.014	18.372 ± 0.009	18.207 ± 0.009	18.518 ± 0.010	19.166 ± 0.015
z	19.413 ± 0.051	18.747 ± 0.034	18.505 ± 0.035	18.860 ± 0.034	19.477 ± 0.058
J		18.511 ± 0.052		18.882 ± 0.178	19.217 ± 0.117
H		19.113 ± 0.198		18.746 ± 0.099	
W1				17.305 ± 0.130	
W2				16.282 ± 0.192	
W3				12.128 ± 0.269	
W4				8.250 ± 0.190	